A. Boudjemaa
S. Tahi
B. Bennamane
T. B. Berbar
B. Lehouidj

J. Electrical Systems x-x (xxx): x-xx

Regular paper

Reflected Signal on a Nonuniform Overhead Transmission Line at High Frequency

The effect of the sag of an overhead transmission line is numerically characterized in the case of two conductors above lossy earth at high frequency. The technique uses the chain ABCD matrix for a transmission line of two conductors above ground and we present a generalized recurrence formulation of the reported input matrix impedance for a finite length section of multiconductor transmission line. Then the nonuniform transmission line can be subdivised into sections of uniform transmission line. This technique is used to calculate input impedance and reflection coefficient of an incurved overhead two-conductor transmission line over the 1-30MHz range.

Keywords: power line communications, multiconductor transmission line, propagation constant, characteristic impedance, quasi-TEM approximation, overhead lines, sag.

1. Introduction

The power line is originally built for power delivery at low frequencies (50 or 60Hz), however it can be used simultaneously as a communication medium at high frequencies (1-30MHz). Then an important research effort is made in many countries to enhance the performance of BPL (Broad band Power Line). One of the important limitations of this communication channel is the multiple reflections that reduce the effective available bandwidth. This work is essentially focused on the reflection coefficient of the incurved overhead two wires transmission line.

It is interesting to know the electrical characteristics of a Multiconductor Transmission Line (MTL) in several configurations. The modal method is introduced in 1926 by J.R. Carson [1] for the industrial frequencies and extended by M. D'Amore & al [2] and R.G. Olsen & al [3] to the high frequency range (1-30MHz). This method is used for the study of coupling between parallel cylindrical conductors (Figure 1) in the frequency domain. Diameter, conductivity and magnetic permeability of each conductor wire are explicitly taken into account, and the influence of electrical and magnetic ground characteristics can be evaluated.

Using the extended method, P. Amirshahi & al [4] show that the transmission capacity of the MTL is very high in ideal and theoretical situation: binary capacity of 1Gbps over 1Km is possible.

In the case of overhead parallel wires, the structure is not strictly TEM because ground and wires are not perfect conductors. However, under some conditions, their behavior is quasi-TEM mode and the radiation is supposed negligible. C.R. Paul [5] clarifies the widely used decoupling technique for the determination of propagation constants and characteristic impedances.

Corresponding author : A. Boudjemaa
Faculté d'Electronique et d'Informatique,Université des Sciences et de la Technologie Houari Boumédiène, Alger-Algérie
Boudjemaa.Abdelkrim@hotmail.com,

In real situation, the overhead transmission line is incurved and the distance between the lowest level of the incurved wire and the ideal straight line is called the sag (fig. 2.a). It is the consequence of dilatation and weight of the conductors[6].

In the situation of a nonuniform MTL, we use method usual in microstrip patches and antennas analysis: impedance matching [7], microstrip patch antenna [8] [9], two-conductor microstrip antenna [9] [11]. The nonuniform MTL is subdivised into elementary uniform MTL then the properties of the chain ABCD matrix can be used for the determination of impedance, voltage, current and power of the considered structure.

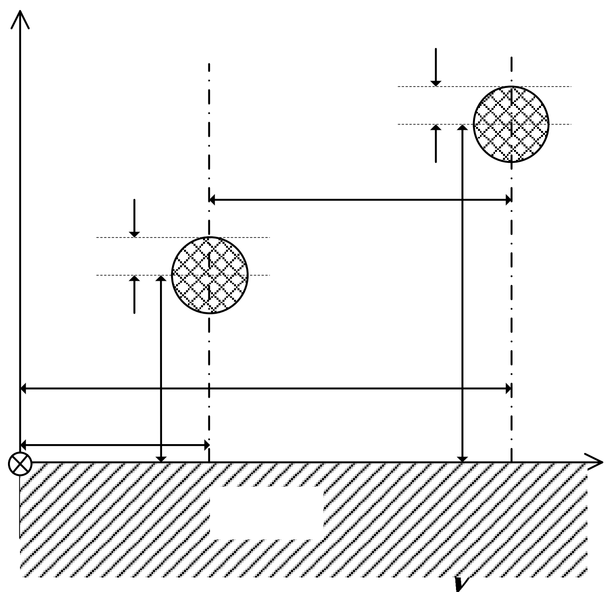

Fig. 1. Parallel Two-conductor transmission line with loss

2. Incurved Two-Conductor Transmission Line

2.1. Description

Voltages and currents waves are propagating along the two conductor transmission lines. Figure 2.b represents the voltages and currents of a set of two coupled parallel conductors, the ground is also a conductor. Where: $\hat{V}(z) = [V_1, V_2]^t$ Vector of phasor line voltage (with respect to the reference ground) at the distance z from the origin, and $\hat{I}(z) = [I_1, I_2]^t$ vector of phasor line current at the distance z from the origin. $\hat{V}_0 = \hat{V}(0)$ and $\hat{I}_0 = \hat{I}(0)$ the voltage and current phasors at the origin.

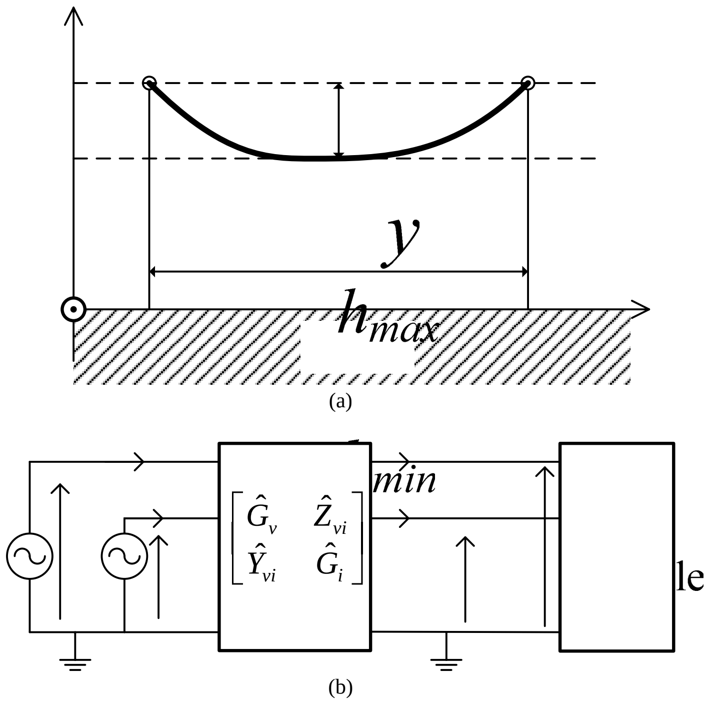

Fig. 2. Overhead two-conductor line with sag. (a) Description. (b) Electrical model

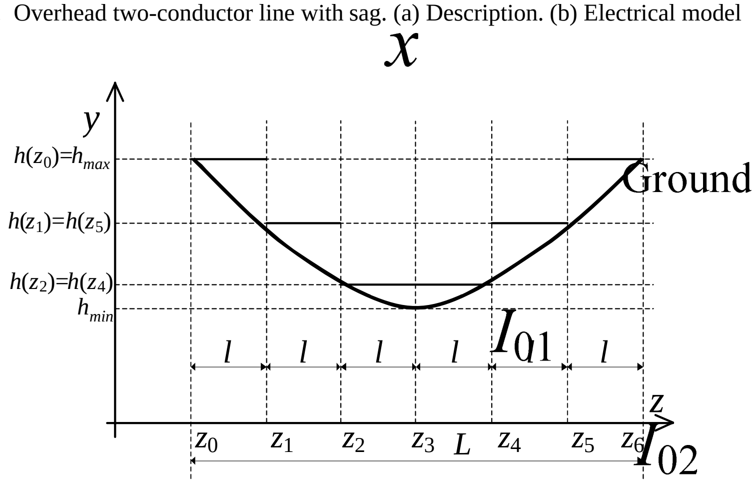

Fig. 3. Subdivision of overhead two-conductor line with sag (N=6)

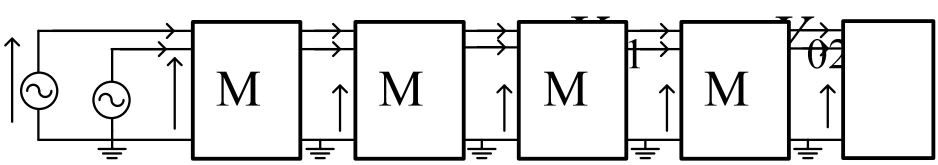

Fig. 4. Electrical model of subdivised two-conductor transmission line (N = 4)

We consider $\hat{Z}_{in}(z)$ the input impedance matrix for any position z along the two-conductor line [5]:

$$\hat{V}(z) = \hat{Z}_{in}(z) \cdot \hat{I}(z) \tag{1.a}$$

At the origin ($z = 0$) we have the following relationship:

$$\hat{V}_0 = \hat{Z}_{in} \cdot \hat{I}_0 \tag{1.b}$$

We can identify the curve of the overhead line (Fig. 2.a) with the following function:

$$h(z) = h_{min} \cosh\left(\operatorname{acosh}(h_{max} / h_{min}) \cdot (2z / L - 1)\right) \tag{2}$$

The incurved line (Fig. 3) is subdivised into N sections of length l that must be a small fraction of the wavelength of the signal. Then the number N and the length l verify the following conditions:

$$N \geq 16L \frac{f_{\max}}{c} \tag{3.a}$$

$$l \leq \frac{c}{16 f_{\max}} \tag{3.b}$$

To have pertinent frequency response, the number N_f of frequency values must verify this condition on the range [$f_{\max}$,$f_{\min}$]:

$$N_f \geq 32L \frac{(f_{\max} - f_{\min})}{c} \tag{4}$$

2.2. ABCD-Matrix for a nonuniform transmission line

The electrical model (Fig. 4) can be formulated as follows:

$$\begin{bmatrix} \hat{V}(L) \\ \hat{I}(L) \end{bmatrix} = \begin{bmatrix} \hat{G}_v & \hat{Z}_{vi} \\ \hat{Y}_{vi} & \hat{G}_i \end{bmatrix}^{-1} \cdot \begin{bmatrix} \hat{V}_0 \\ \hat{I}_0 \end{bmatrix} \tag{5.a}$$

$$\begin{bmatrix} \hat{G}_v & \hat{Z}_{vi} \\ \hat{Y}_{vi} & \hat{G}_i \end{bmatrix}^{-1} = \prod_{m=N}^{1} \mathrm{M}_m^{-1} \tag{5.b}$$

$$\mathrm{M}_m^{-1} = \begin{bmatrix} \hat{A}_m & -\hat{B}_m \cdot \hat{Z}_C(h_m) \\ -\hat{Y}_C(h_m) \cdot \hat{B}_m & \hat{Y}_C(h_m) \cdot \hat{A}_m \cdot \hat{Z}_C(h_m) \end{bmatrix} \tag{5.c}$$

$$\hat{A}_m = \cosh\left(l \ \hat{\gamma}(h_m)\right) \tag{5.d}$$

$$\hat{B}_m = \sinh\left(l \ \hat{\gamma}(h_m)\right) \tag{5.e}$$

$\hat{\gamma}$: Propagation matrix

$\hat{Z}_C$: Characteristic impedance matrix of the MTL

$\hat{Y}_C = \hat{Z}_C^{-1}$: Characteristic admittance matrix of the MTL

The elements of the propagation and the characteristic impedance matrices are calculated using the formulas presented by [2] and used by [4] under the usual quasi-TEM restrictions: $d << \lambda$, $h_i << \lambda_w$, $a_i << h_i$, $a_i << d$ (Fig. 1).

Where λ and λ_w denote wavelengths in vacuum and in conductors respectively.

We notice that hyperbolic sin and cos of matrices appears in (5.d) and (5.e), the author of [12] presented powerful and efficient numerical algorithm to calculate them.

2.3. Recurrence impedance relationship

They are evaluated with the following recurrence expressions. Starting with the right extremity (Fig. 4), a matched load is connected at interface $N + 1$:

$$\hat{Z}_{N+1} = \hat{Z}_L = \hat{Z}_C(h_{\max}) \tag{6}$$

Then, we compute successively the input impedance at each interface as follow (index m is decremented from $N + 1$ to 1):

$$\hat{Z}_{m-1} = \hat{X}_m \cdot \hat{Y}_m^{-1} \cdot \hat{Z}_{C,m-1} \tag{7.a}$$

$$\hat{X}_m = \hat{A}_{m-1} \cdot \hat{Z}_m + \hat{B}_{m-1} \cdot \hat{Z}_{C,m-1} \tag{7.b}$$

$$\hat{Y}_m = \hat{B}_{m-1} \cdot \hat{Z}_m + \hat{A}_{m-1} \cdot \hat{Z}_{C,m-1} \tag{7.c}$$

This step is repeated until we reach the feed location where ($m = 1$) $\hat{Z}_{in} = \hat{Z}_1$.

2.4. Input impedances and reflection coefficients

The attenuation of the two-conductor transmission line can be deduced by comparing the total active power P_{in} entering into the system with the power P_L flowing into the load.

The input impedance matrix derived from recurrent relation (7) can be written:

$$\hat{Z}_{in} = \begin{bmatrix} Z_{in11} & Z_{in12} \\ Z_{in21} & Z_{in22} \end{bmatrix} \tag{8}$$

From Figure 5.a, the common mode input impedance is defined as:

$$Z_{inc} = \frac{V}{I} \tag{9}$$

Where $V = V_{01} = V_{02}$ and $I = I_{01} + I_{02}$

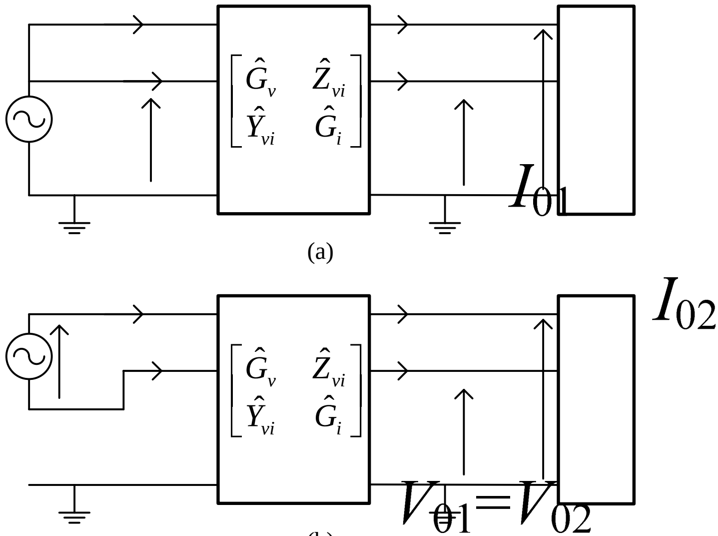

Fig. 5. Excitation mode of the MTL. (a) Common mode. (b) Differential mode.

Moreover, from Figure 5.b, the differential mode input impedance is defined as:

$$Z_{ind} = \frac{V_{Dif}}{I} \tag{10}$$

Where $V_{Dif} = V_{01} - V_{02}$ and $I = I_{01} = -I_{02}$

Finally, the expression of the common and differential mode input impedances are respectively:

$$Z_{inc} = \frac{Z_{in11} Z_{in22} + Z_{in12} Z_{in21}}{Z_{in11} + Z_{in22} - Z_{in12} - Z_{in21}} \tag{11.a}$$

$$Z_{ind} = Z_{in11} + Z_{in22} - Z_{in12} - Z_{in21} \tag{11.b}$$

The reference impedance matrix is:

$$\hat{Z}_N = \begin{bmatrix} Z_{N11} & Z_{N12} \\ Z_{N21} & Z_{N22} \end{bmatrix} \tag{12}$$

Common and differential mode reference impedances are respectively:

$$Z_{Nc} = \frac{Z_{N11} Z_{N22} + Z_{N12} Z_{N21}}{Z_{N11} + Z_{N22} - Z_{N12} - Z_{N21}} \tag{13.a}$$

$$Z_{Nd} = Z_{N11} + Z_{N22} - Z_{N12} - Z_{N21} \tag{13.b}$$

The reference impedance matrix can be chosen arbitrary but the better choice is the characteristic impedance matrix of the first segment of the MTL.

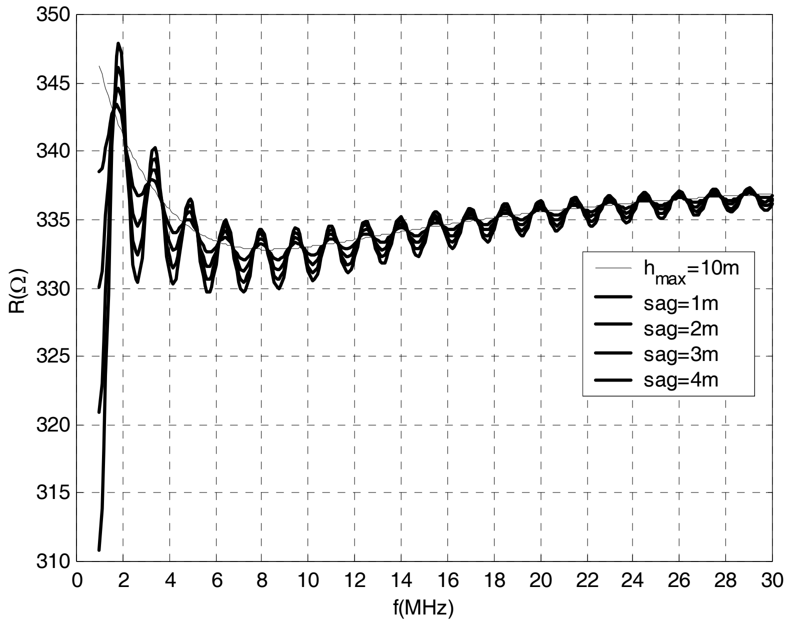

(a)

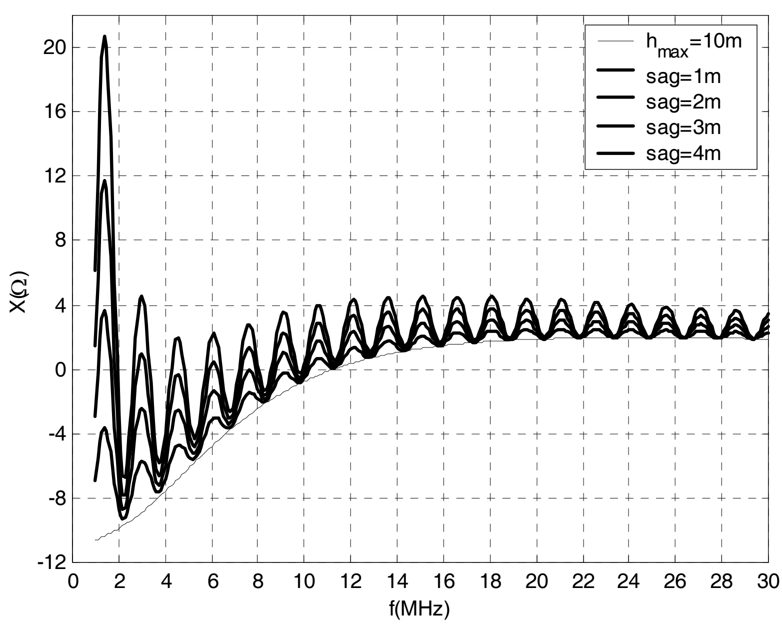

(b)

Fig. 6. Common mode input impedance of the two-conductor line above ordinary soil. (a) Resistance. (b) Reactance.

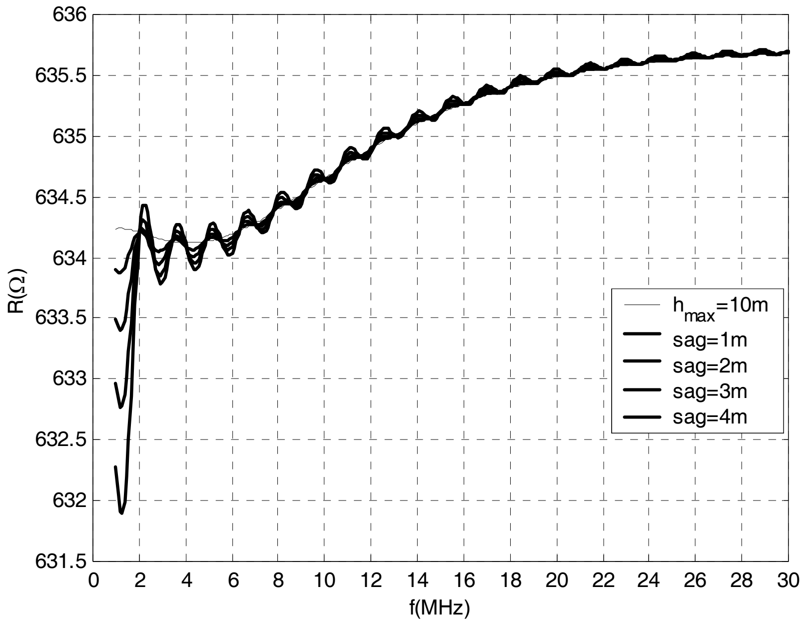

(a)

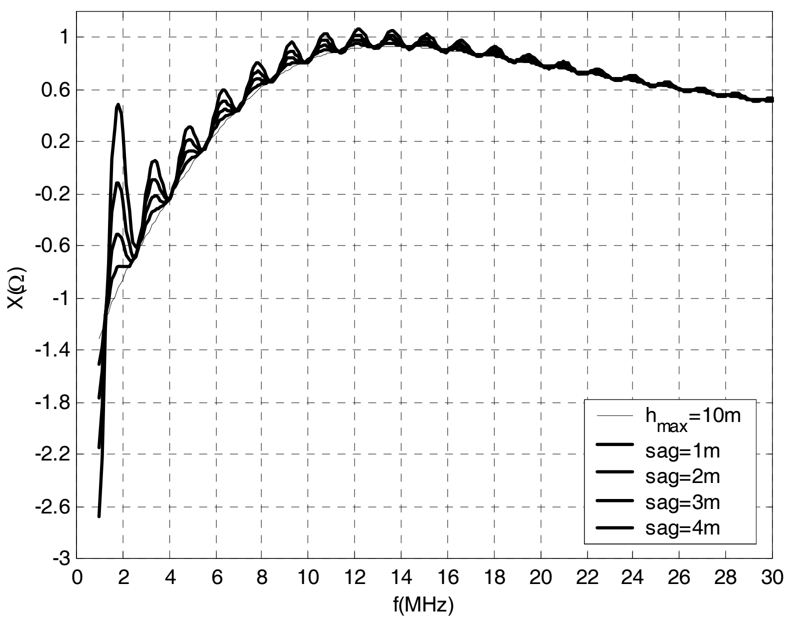

(b)

Fig. 7. Differential mode input impedance of the two-conductor line above ordinary soil. (a) Resistance. (b) Reactance.

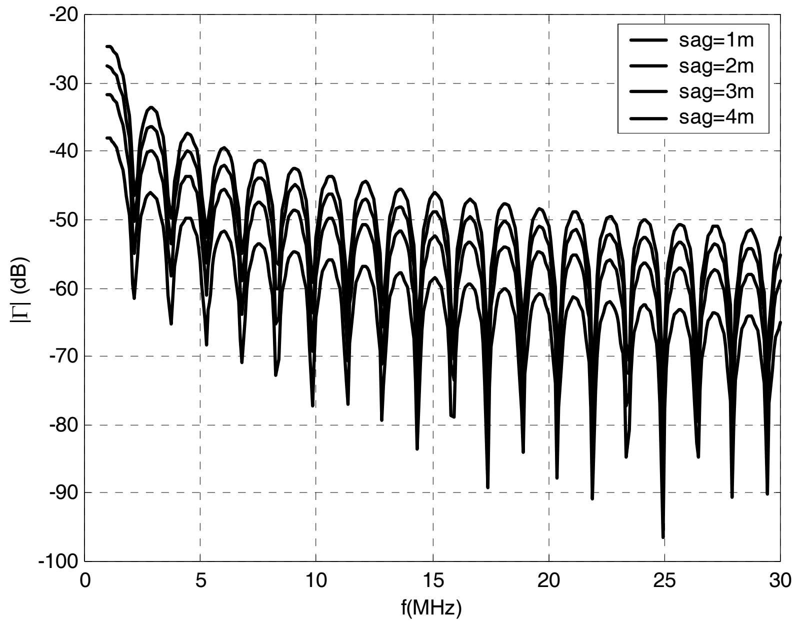

(a)

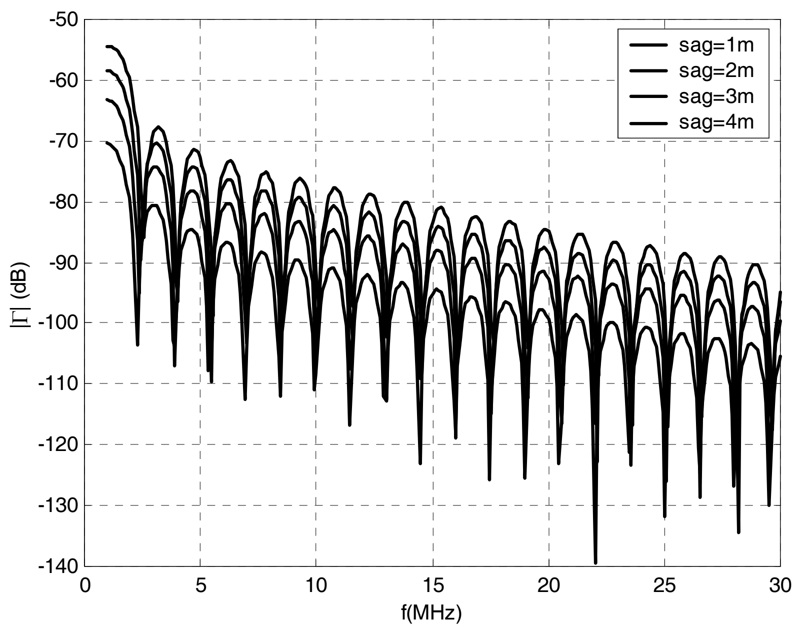

(b)

Fig. 8. Reflection coefficient of the two-conductor line above ordinary soil. (a) Common mode. (b) Differential mode.

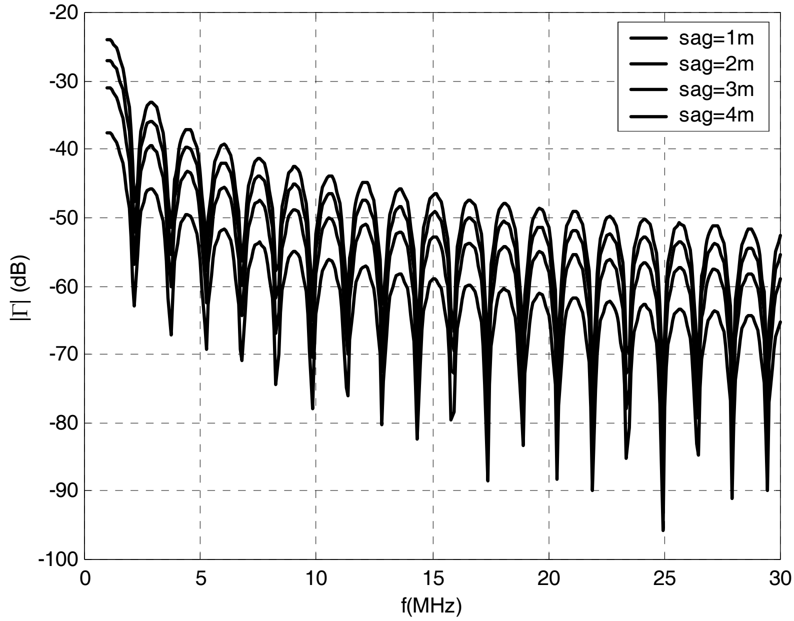

(a)

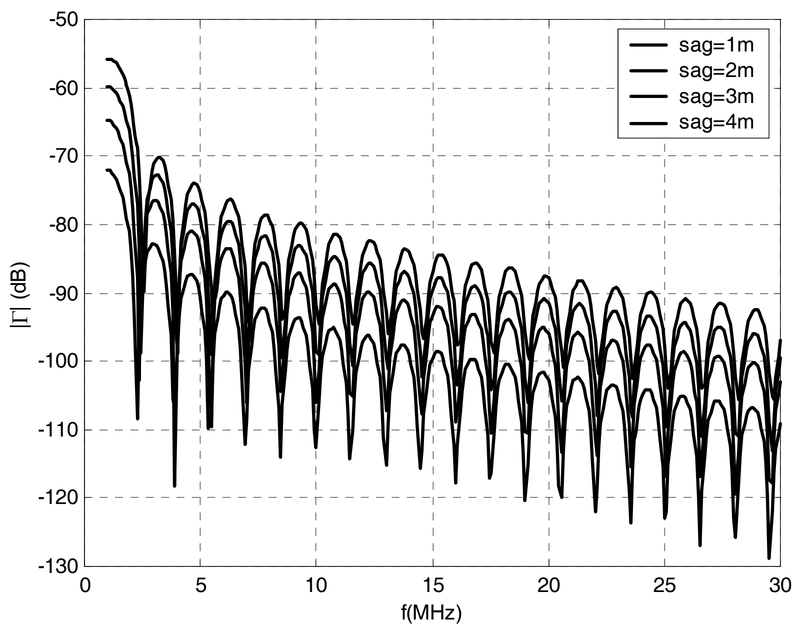

(b)

Fig. 9. Reflection coefficient of the two-conductor line above wet soil. (a) Common mode. (b) Differential mode.

Then, the common and differential reflection coefficients are respectively:

$$\Gamma_c = \frac{Z_{inc} - Z_{Nc}}{Z_{inc} + Z_{Nc}} \quad (14.a)$$

$$\Gamma_d = \frac{Z_{ind} - Z_{Nd}}{Z_{ind} + Z_{Nd}} \quad (14.b)$$

These expressions are used to study lines that have a curvature, it becomes then easy to quantify the effect of the sag of an overhead line on the frequency response.

3. Numerical application

A numerical application is made to quantify the effect of the sag at high frequency. During simulation, it is assumed in all cases, spacing between wires is d = 1m, the maximal height of the wires is equal to h_{max} = 10m, and the transmission line has a span of L = 100m. We consider average (σ_g = 0.005S/m, ε_g = 13) and wet (σ_g = 0.01S/m, ε_g = 30) soils. The results for common and differential modes are presented.

In the case of ordinary soil, we compare (Fig. 6 and 7) the input impedance of the uniform straight line (h_{max} = 10m) with that of the incurved line for many values of the sag (1, 2, 3 and 4 m). Oscillations appear for the input impedance in the curved line case. This effect is more pronounced for a large sag. But it is less important for the differential mode (Fig. 7).

The figures 8 and 9 show respectively the reflection coefficient for an ordinary and a wet soils. We notice that the soil characteristic has a negligible effect on the reflection coefficient. However, the latter is less than -20dB for the common mode and -50dB for the differential mode. It is concluded that the reflection coefficient increases with the sag.

This work clearly shows that the sag of an overhead line has a significant influence on the reflection coefficient and therefore on the useful bandwidth at high frequencies (1 to 30 MHz) of a signal transmitted over this kind of line.

References

[1] J.R. Carson, "Wave propagation in overhead wires with ground return", *Bell Syst. Techn. Journal*, Vol.5, 1926, pp.539-554

[2] M. D'Amore, M.S. Sarto, "A New Formulation of Lossy Ground Return Parameters for Transient Analysis of Multi-Conductor Dissipative Lines", *IEEE-T-Power Del*., Vol.12, n°1, January 1997, pp.303-314

[3] R.G. Olsen, M.D. Wu, " High Frequency Propagation Losses on an Open Wire Transmission Line Above Dissipative Earth", *IEEE-T-Broadcast*., Vol.34, n°2, June 1988, pp.292-300

[4] P. Amirshahi, M. Kavehrad, "High-Frequency Characteristics of Overhead Multiconductor Power Lines for Broadband Communications", IEEE Journal on Selected Areas in Communications, Vol.24, n°7, July 2006, pp.1292-1303

[5] C.R. Paul, "Decoupling the Multiconductor Transmission Line Equations", IEEE-T-MTT, Vol.44, n°8 , August 1996, pp.1429-1440

[6] M. Muhr, S. Pack, R. Schwarz, S. Jaufer, "Calculation of Overhead Line Sags", 51st *Internationales Wissenschaftliches Kolloquium, Technische Universität Ilmenau, 11-15 September 2006*

[7] S.J. Orfanidis, Electromagnetic Waves and Antennas , Rutger University, USA, 2008

[8] G. Dubost, "Linear Transmission Line Model Analysis of Arbitrary Shape Patch Antenna", Electronics

Letters Vol.22, N°15, 17 July 1986, pp.798-799.

[9] T.B. Berbar, A. Mokraoui, A. Zerguerras, R. Aksas, “Experimenting FCEL Method on Dropelike-Shaped Microstrip Patch Antenna”, Microwave and Optical Technology Letters, August 2006, Vol.48, N°8, pp.1495-1498.

[10] G. Dubost, A. Zerguerras, “Transmission Line Model Analysis of Arbitrary Shape Symmetrical Patch Antenna Coupled with a Director”, *Electronics Letters* Vol.26, N°13, 21st June 1990, pp.952-954.

[11] T.B. Berbar, A. Azrar, A. Zerguerras, R. Aksas, “Application of the FCEL method to a microstrip disk antenna with a parasitic director”, Microwave and Optical Technology Letters, August 2009, Vol.51, N°8, pp.1911-1918.

[12] N.J. Higham, Functions of Matrices: Theory and Computation, SIAM, Philadelphia, PA, USA, 2008